# Increased cell compaction can augment the resistance of HT-29 human colon adenocarcinoma spheroids to ionizing radiation

ANTONELLA FERRANTE[1], GABRIELLA RAINALDI[1,2], PAOLA INDOVINA[1], PIETRO LUIGI INDOVINA[2,3] and MARIA TERESA SANTINI[1,2]

[1]Dipartimento di Ematologia, Oncologia e Medicina Molecolare, Istituto Superiore di Sanità, Viale Regina Elena 299, I-00161 Rome; [2]Istituto Nazionale per la Fisica della Materia, Unità di Napoli, [3]Dipartimento di Scienze Fisiche, Università di Napoli 'Federico II', Complesso Universitario Monte S. Angelo, Via Cinthia, I-80126 Naples, Italy

Received June 8, 2005; Accepted July 9, 2005

**Abstract.** One of the most important questions in tumor biology is the understanding of the mechanisms responsible for the resistance of cancer cells to radiotherapy. In the present study, the possible role played by cell-cell interactions in determining the response of tumor cells to ionizing radiation was investigated. HT-29 colon adenocarcinoma spheroids were irradiated with a dose of 15 Gy in two different stages of growth characterized by diverse degrees of compaction: loosely organized spheroids (early spheroids) and compacted spheroids (late spheroids). Morphological analyses demonstrated that late spheroids were less damaged than early spheroids. Moreover, analyses of the cell cycle and cell death showed that ionizing radiation induced necrosis in early spheroids and apoptosis in late ones. From these results it can be concluded that late, compacted spheroids are more resistant to ionizing radiation than early, loose spheroids. In order to understand the mechanisms regulating this compaction-induced resistance of late spheroids, E-cadherin/ß-catenin complex expression and distribution were analyzed. In late spheroids, E-cadherin/ß-catenin complexes were shown to be tethered to the cytoskeleton, and since this organization has been demonstrated to strengthen cell-cell adhesion in other systems, it can be postulated that the same is true in HT-29 spheroids. In conclusion, it can be hypothesized that compaction of HT-29 spheroids is mediated by the reorganization of E-cadherin/ß-catenin complexes on the plasma membrane and that this compaction may be responsible for the increase in resistance of HT-29 spheroids to ionizing radiation.

*Correspondence to:* Dr Maria Teresa Santini, Dipartimento di Ematologia, Oncologia e Medicina Molecolare, Istituto Superiore di Sanità, Viale Regina Elena 299, I-00161 Rome, Italy
E-mail: santini@iss.it

*Key words:* three-dimensional tumor spheroids, ionizing radiation, compaction, cell adhesion molecules, E-cadherin

## Introduction

In order to better comprehend tumor cell biology, it is necessary to utilize *in vitro* models that are able to represent *in vivo* tumors as precisely as possible. Conventional monolayer cultures used in cancer research are not completely representative of the complex microenvironmental conditions and the intricate cell-cell interactions found in solid tumors. In fact, it appears evident that the bi-dimensional organization of cells in monolayer is completely different from the three-dimensional structure of solid tumors. Moreover, the homogeneous exposure to nutrients and oxygen typical of cells grown in monolayer is not representative of the heterogeneous distribution of these substances in *in vivo* tumors. In an attempt to overcome the experimental restrictions of monolayer cultures, in the early 1970s three-dimensional multicellular spheroids were developed. The three-dimensional organization of cells in spheroids mimics quite faithfully the intercellular interactions and the close communications between cells in solid tumors. Furthermore, this particular organization results in the development of quiescent and hypoxic (sometimes necrotic) cells in the inner zones of spheroids similar to those found in tumors. The closer resemblance of spheroids to tumors is also illustrated by the fact that multicellular spheroids respond to antineoplastic stimuli in a different manner than monolayers (1,2). In particular, it has been shown that spheroids are more resistant to chemical (antitumor drugs) and physical (ionizing radiation) agents than monolayers and that this resistance is comparable to the one found in *in vivo* tumors (3). Therefore, it can be theorized that studying this three-dimensional model can help elucidate the physiological, cellular and molecular mechanisms of resistance in cancer, one of the most important questions in tumor biology.

Among the various hypotheses that have been formulated in order to explain the different response of monolayer cells and spheroids to stressing agents, the role of cell-cell interaction and cell communication are considered particularly important. It has been suggested that cell-cell contact could supply survival and protective advantages in cells grown as three-dimensional spheroids (4). Although the molecular mechanisms of this phenomenon are not well understood, it appears evident

that cell adhesion molecules (CAMs), which help determine the three-dimensional array of spheroids, could have a pivotal role (4-6). Cell-cell and cell-matrix contacts mediated by CAMs are decisive for cells in sensing environmental stimuli and, consequently, in transducing signals for cell survival.

With this in mind, it was the purpose of the present study to investigate the role played by cell compaction in regulating the response of spheroids to a stressing agent. Consequently, spheroids with different degrees of cell-cell contact were used. Specifically, HT-29 human colon adenocarcinoma spheroids at two different stages of growth were utilized: early spheroids (24 h) with weaker cell-cell contacts which formed loose spheroids and late spheroids (72 h) with stronger cell-cell contacts which formed well-compacted ones. The influence of cell-cell contact in the two spheroid models was investigated using gamma radiation (15 Gy). After 48 h from irradiation, morphology (light and electron microscopy), cell cycle distribution (flow cytometry), cell death (Hoechst staining) and E-cadherin/ß-catenin expression (Western blotting) were analyzed. The results reveal that early spheroids were morphologically more damaged by ionizing radiation than late ones. In addition, early spheroids died of necrosis while late spheroids died by apoptosis, a regulated type of death. E-cadherin/ß-cateninn analysis revealed a different distribution of these two important proteins in the two spheroid models. In fact, with respect to early spheroids, late spheroids presented much more E-cadherin connected to the cytoskeleton through the engagement of ß-catenin. This observation suggests that the stronger compaction of late spheroids is due to the re-distribution of E-cadherin on the plasma membrane and possibly to the interaction of this protein with its cytoplasmic partner ß-catenin.

## Materials and methods

*Cell cultures*. All experiments were performed with the human colon adenocarcinoma cell line HT-29 (obtained from the Istituto Zooprofilattico Sperimentale della Lombardia e dell'Emilia, Brescia, Italy). Cells were grown in monolayer in RPMI-1640 medium (Gibco BRL, Burlington, ON, Canada) supplemented with 10% fetal bovine serum (FBS Characterized; Hyclone, USA), 1% non-essential amino acids (Gibco), 100 IU/ml penicillin (Gibco) and 100 $\mu$g/ml streptomycin (Gibco) and incubated at 37˚C in a 5% $CO_2$ atmosphere.

*Multicellular tumor spheroids*. In order to obtain spheroids, the liquid-overlay technique was used. HT-29 cells, detached from the substratum by adding 10 mM EDTA (pH 7.4) and 0.25% trypsin, were then seeded in Petri dishes to which 3% agar dissolved in complete medium (RPMI plus 10% FBS) had previously been added to the bottom of the wells and had solidified. Each Petri dish was seeded with $1.0x10^5$ cells/ml and incubated at 37˚C in a 5% $CO_2$ atmosphere.

*Irradiation protocol*. Spheroids were irradiated after 24 h (early spheroids) and 72 h (late spheroids) of growth directly in the tissue culture dishes at room temperature with a single dose of 15 Gy using a Cobalt-60 irradiation unit (Gammacell 220, Atomic Energy of Canada Ltd.) at a dose rate of ~12.2 Gy/min. Control spheroid cultures were kept at room temperature under the same conditions as experimental ones. After irradiation, the cultures were returned to incubate and were collected at the appropriate times for the experiments described below.

*Light microscopy*. In order to evaluate the morphology of HT-29 early and late spheroids, they were observed and photographed directly in the Petri dishes using an inverted Zeiss Axiovert light microscope.

*Semithin sections*. In order to evaluate the compaction degree of early and late spheroids and the cellular damage induced 48 h from irradiation, semithin sections were analyzed. Spheroids were collected from the dishes, placed in 15 ml tubes and centrifuged at 300 x g for 3 min. The supernatant was removed and the spheroids were fixed with 2.5% glutaraldehyde in 0.1 M cacodylate buffer (pH 7.4) at room temperature for 30 min. After washing twice with the same buffer, the samples were post-fixed in 1% osmium tetroxide for 30 min at room temperature, dehydrated through graded ethanols up to 70%. The samples were then contrasted with a filtered, saturated solution of uranyl acetate in 70% ethanol at room temperature for 30 min in the dark. Dehydration was completed through graded ethanols up to absolute ethanol. Samples were placed in a propylene oxide solution for 20 min at room temperature, embedded in epoxy resin (TAAB T004, Balzers) and polymerized for 48 h at 60˚C. Semithin section were obtained with an ultramicrotome (LKB, Nova), stained with toluidine blue (pH 8.0) and observed with an inverted Zeiss Axiovert light microscope.

*Scanning electron microscopy (SEM)*. In order to analyze morphologically the radiation-induced damage, early and late spheroids were observed 48 h from irradiation utilizing SEM. They were collected from the dishes, placed in 15 ml tubes and centrifuged at 300 x g for 3 min. The supernatant from the tubes containing the spheroids was removed and the spheroids were seeded on glass coverslips coated with polylysine for 30 min at room temperature. Spheroids were then fixed with 2.5% glutaraldehyde in 0.1 M cacodylate buffer (pH 7.4) at room temperature for 30 min. After washing twice with the same buffer, the samples were post-fixed in 1% osmium tetroxide for 30 min at room temperature, dehydrated through graded ethanols, critical point dried in $CO_2$ and gold coated by sputtering. The samples were examined with a Cambridge 360 scanning electron microscope.

*Cell cycle analysis*. The cell cycle phase distribution ($G_0/G_1$, S and $G_2$/M) of early and late spheroids was determined 24, 48 and 72 h from irradiation. In order to obtain a single-cell suspension, it was first necessary to disaggregate the spheroids. The spheroids were collected from the dishes, placed in 15 ml tubes, centrifuged at 300 x g for 3 min and the supernatant removed. The spheroids were disaggregated by gentle pipetting for about 2 min after adding 1 ml of 10 mM EDTA and 2 ml of 0.25% trypsin, both at a temperature of 37˚C. Trypsin action was then stopped by adding medium containing 10% FBS. The single-cell suspension obtained was fixed in ice-cold 70% ethanol for at least 10 min. Subsequently, cells were centrifuged and then resuspended

in PBS containing 50 $\mu$g/ml of the DNA fluorescent probe propidium iodide (PI) and incubated for 1 h at room temperature. Fluorescence was analyzed with a FACScan flow cytometer (Becton Dickinson, Mountain View, CA, USA) equipped with a 15 mW, 488 nm, air-cooled argon ion laser. Fluorescence emissions were collected after passage through a 530 nm band-pass filter for PI. A minimum of at least 5,000 events were acquired in list mode using the CellQuest® software (Becton Dickinson). Forward (FSC) and side (SSC) scatter were collected as linear signals and fluorescence emissions were collected on a linear scale. Doublets and aggregates were gated on the dot-plot: PI fluorescence peak versus PI fluorescence area. Cell cycle analysis was conducted using the Sfit model included in the CellFit® software (Becton Dickinson).

*Hoechst staining*. In order to obtain quantitative information on the number of necrotic and apoptotic cells, the nuclei of cells from dissociated spheroids were stained after 48 h from irradiation with the chromatin dye Hoechst 33258 (Sigma, St. Louis, MO, USA) and observed by light fluorescent microscopy. Briefly, the single cell suspension obtained from the spheroids was fixed with 3.7% paraformaldehyde in PBS for 15 min. The cell pellets were then placed on polylysine-coated coverslips and allowed to adhere for 20 min, permeabilized with 0.5% Triton X-100 in PBS for 5 min and incubated with 1 $\mu$g/ml Hoechst 33258 for 30 min at 37˚C. The samples were mounted on glass coverslips with a glycerol/PBS mixture, and observed and photographed with a Zeiss Axiovert fluorescence microscope. The percentage of necrotic and apoptotic cells obtained from control and irradiated MG-63 spheroids was determined by counting at high magnification (x500) at least 500 cells of each sample in randomly selected areas. In order to distinguish apoptotic and necrotic cells, the nuclear morphological and ultrastructural parameters typical of these two kinds of cell death were taken into account (7-9).

*Western blotting*. In order to analyze the expression of $B_1$-cyclin, E-cadherin and ß-catenin proteins, whole cell extracts of early and late spheroids were prepared. Briefly, spheroids were collected, washed twice in PBS and lysed in RIPA buffer (PBS containing 1% Igepal CA-630, 0.5% sodium deoxycholate, 0.1% SDS, 0.1 mg/ml PMSF and protease inhibitor cocktail) for 30 min on ice. The lysates were centrifuged at 10,000 x g for 10 min at 4˚C and the pellets were discarded.

In order to analyze the different distribution of E-cadherin and ß-catenin in cells composing early and late spheroids, the Sasaki *et al* protocol was followed (10). Briefly, spheroids were rinsed twice in PBS (pH 7.4) and incubated on ice in Triton X-100 buffer [1% Triton X-100, 10 mM Tris-HCl (pH 7.5), 140 mM NaCl, 5 mM EDTA, 2 mM EGTA, 1 mM PMSF; 1 $\mu$g/ml aprotinin] for 30 min. They were disrupted using a 27 Gauge syringe. The lysate was centrifuged at 14,000 x g for 30 min at 4˚C. The supernatant was considered as the TX-100 soluble fraction which contains cytoplasmic and membrane proteins. The pellet was solubilized in SDS/Urea buffer (1% SDS, 8 M urea, 10 mM Tris-HCl (pH 7.5), 5 mM EDTA, 2 mM EGTA, 1 mM PMSF; 1 $\mu$g/ml aprotinin) and is considered as the TX-100 insoluble fraction which contains cytoskeletal and nuclear proteins.

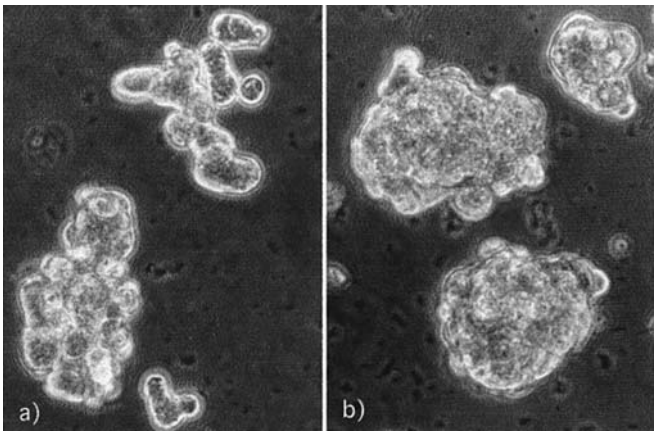


Figure 1. Representative light micrographs of early (a) and late (b) HT-29 spheroids. As can be seen, early spheroids are loosely organized and single cells can be distinguished from each other whereas late spheroids form compacted aggregates that have a well-rounded shape. Individual cells cannot be recognized. Original magnification x1,250.

Protein analyses were conducted by the DC protein assay kit (Bio-Rad Laboratories, Milan, Italy) using BSA as standard. Typically, 50 $\mu$g of protein were boiled in 10X SDS-sample buffer for 3 min, separated onto an 8% SDS-polyacrylamide gel and transferred to the PVDF membrane (Bio-Rad Laboratories). After electroblotting the membranes were blocked with 5% non-fat dry milk (Bio-Rad Laboratories) in TBST (0.1 M Tris base, 0.15 M NaCl, 0.05% Tween-20, pH 7.4) and then incubated with the primary mouse antibodies against $B_1$-cyclin (Chemicon, Milan, Italy), E-cadherin (clone 36, BD Transduction Laboratories, Milan, Italy), ß-catenin (Chemicon) and actin (Chemicon) overnight at 4˚C. Following incubation with an HRP-linked whole anti-mouse antibody (Amersham Biosciences, Milan, Italy), visualization of the bound antibody was performed with the Supersignal West Pico Chemiluminescent Substrate (S.I.A.L., Rome, Italy). The blots were exposed to X-ray film (Amersham Biosciences).

*Statistical analyses*. All statistical analyses not specified were carried out using the paired Student's t-test.

## Results

*Evaluation of spheroid compaction*. As can be seen in Fig. 1a, early spheroids (24 h of growth) are organized in loose aggregates in which individual cells can be recognized. Conversely, late spheroids (72 h of growth) (Fig. 1b) form compacted aggregates that have a well-rounded shape. Semithin sections also show differences in cell organization in early (Fig. 2a) and late (Fig. 2b) spheroids. Cells in early spheroids are much larger and are organized more loosely than cells in late ones.

*Morphological analysis of radiation-induced damage*. At 48 h after irradiation, early and late spheroids were observed by SEM (Fig. 3). Control early spheroids after 72 h of growth (Fig. 3a) appear well-formed and individual cells can be distinguished. These cells appear as bulges on the spheroid

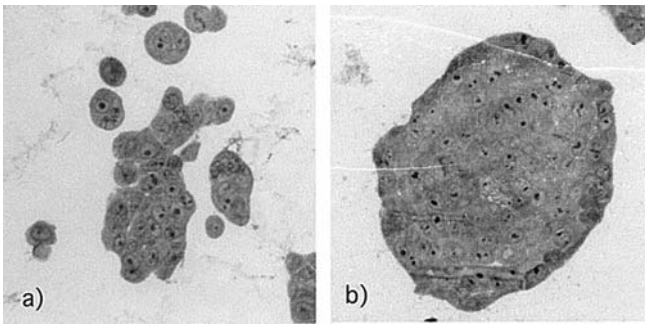


Figure 2. Representative light micrographs of semithin sections of early (a) and late (b) HT-29 spheroids. As can be seen, cells in early spheroids are much larger and are organized more loosely than cells in late spheroids. Original magnification x1,200.

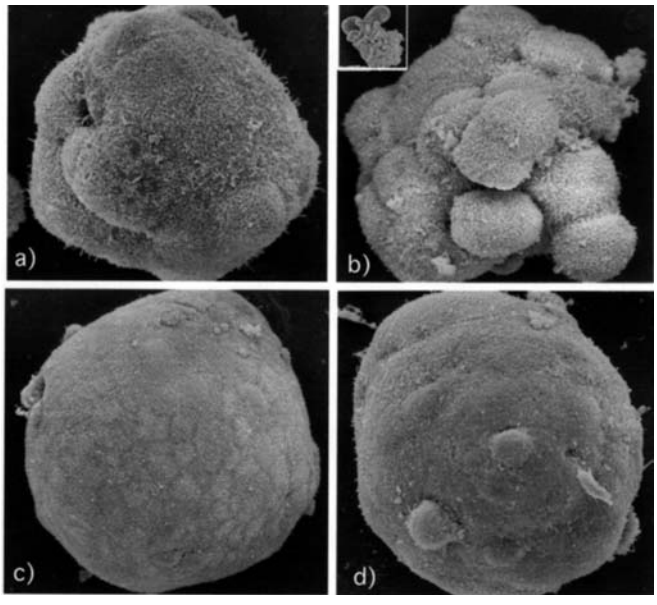


Figure 3. Representative electron micrographs of control early HT-29 spheroids after 72 h of growth (a) and of these spheroids after 48 h of irradiation (b). In (c) and in (d) are shown, respectively, control late HT-29 spheroids after 5 days of growth and these spheroids after 48 h of irradiation. Control early spheroids (a) appear well-formed and individual cells can be distinguished on the surface. Early spheroids after 48 h of irradiation (b) are characterized by numerous cells that are detaching from the spheroid body. In the insert on the top left of Fig. 3b, one of the detached cells is shown. The membrane protrusions ('blebs') on the cell surface are indicative of the great damage induced by ionizing radiation. On the other hand, control late spheroids (c) appear very tightly compacted and smooth on the surface. This morphology is very well-conserved in late spheroids 48 h after irradiation (d) which show no signs of radiation-induced damage. Original magnification: (a), x980; (b), x670; (c), x420; (d), x560; insert, x490.

surface. Early spheroids after 48 h from irradiation (Fig. 3b) are characterized by numerous cells that are detaching from the spheroid body. In the insert on the top left of Fig. 3b, one of these detached cells is shown. The membrane protrusions ('blebs') on the cell surface are indicative of the great damage induced by ionizing radiation. On the other hand, control late spheroids appear very tightly compacted and smooth on the surface (Fig. 3c). This morphology is very well-conserved in late spheroids 48 h from irradiation (Fig. 3d) which show no signs of radiation-induced damage.

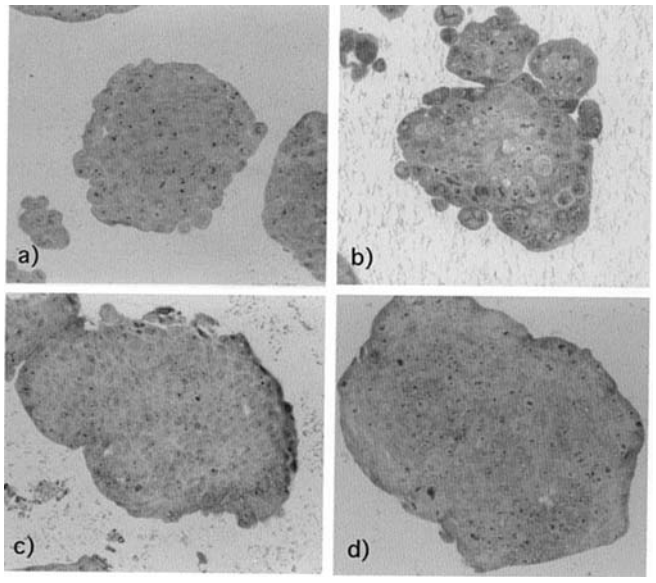


Figure 4. Representative light micrographs of semithin sections of control early spheroids (a) after 72 h of growth and of these spheroids after 48 h of irradiation (b). In (c) and in (d) are shown semithin sections from control late HT-29 spheroids after 5 days of growth and from these spheroids after 48 h of irradiation, respectively. Control early spheroids (a) appear well-organized and consist of small cells with uniform shape. On the other hand, in early spheroids 48 h after irradiation (b), many single cells and clusters of cells can be seen detaching from the spheroid. Furthermore, numerous cells in these spheroids appear enlarged and have a non-uniform shape. As can be seen, after 48 h of irradiation late spheroids (d) appear quite similar to their controls (c). Original magnification x660.

Analysis of semithin sections also confirms these data (Fig. 4). In fact, in early spheroids 48 h from irradiation (Fig. 4b), many single cells and clusters of cells are detaching from the spheroid. Furthermore, numerous cells in spheroids appear enlarged and have a non-uniform shape. These features are indicative of the great damage induced by ionizing radiation and are particularly evident if early spheroids are compared to their controls (Fig. 4a).These spheroids appear well-organized and are formed by small cells with uniform shape. In Fig. 4c and d, respectively, control and irradiated late spheroids are shown. As can be seen in Fig. 4d, 48 h from irradiation, spheroids appear quite similar to their controls (Fig. 4c) and, above all, they do not show signs of the damage that was evident in early-irradiated spheroids (Fig. 4b).

*Cell cycle analysis*. Ionizing radiation often induces cell cycle arrest in either the $G_0/G_1$ or $G_2/M$ checkpoints. In order to assess its effects on early and late spheroids, flow cytometry was performed. In Table IA, the percentages of control and irradiated cells from early spheroids in the $G_0/G_1$, S and $G_2/M$ phases of the cell cycle are shown. Even if irradiated cells show a different cell cycle phase distribution with respect to their controls, no signs of cell cycle arrest are present. However, late spheroids (Table IB) show an evident $G_2/M$ arrest beginning at 24 h after irradiation (i.e., 4 days of growth). Cell cycle arrest was also confirmed by Western blot analysis of $B_1$-cyclin (Fig. 5). After 24 h and 48 h from irradiation (Fig. 5, lanes 2 and 4, respectively), late spheroids show an accumulation of $B_1$-cyclin protein indicative of $G_2$ cycle arrest (11). Conversely, control spheroids after 4 and 5

Table I. Cell cycle phase ($G_0/G_1$, S, $G_2/M$) distributions of cells in control and irradiated early spheroids (A) and in control and irradiated late spheroids (B).[a]

| A, Early spheroids | Time of growth (h) | $G_0/G_1$ (%) | S (%) | $G_2/M$ (%) |
|---|---|---|---|---|
| Control | 0 | 50.3±4.2 | 46.4±3.2 | 2.6±0.1 |
| | 24 | 32.8±4.1 | 30.6±3.3 | 36.6±4.2 |
| | 48 | 52.8±5.9 | 35.6±5.0 | 11.6±2.1 |
| | 72 | 60.2±6.4 | 27.7±2.8 | 12.1±1.4 |
| | 96 | 75.9±5.3 | 19.7±2.2 | 4.4±0.8 |
| 15 Gy | 0 | 50.3±4.2 | 46.4±3.2 | 2.6±0.1 |
| | 24 | 28.1±4.3 | 50.3±5.1 | 21.6±3.4 |
| | 48 | 20.9±3.5 | 24.3±2.8 | 54.8±6.1 |
| | 72 | 35.8±4.2 | 19.2±1.5 | 44.9±4.2 |
| | 96 | 31.4±2.3 | 33.5±1.3 | 35.1±3.0 |
| B, Late spheroids | Time of growth (days) | $G_0/G_1$ (%) | S (%) | $G_2/M$ (%) |
| Control | 0 | 52.6±5.2 | 37.4±3.5 | 10.1±0.8 |
| | 3 | 55.4±5.3 | 32.3±4.2 | 12.3±1.3 |
| | 4 | 68.1±6.1 | 18.8±4.0 | 13.1±3.2 |
| | 5 | 68.3±5.4 | 26.2±3.4 | 5.5±0.5 |
| | 6 | 77.0±4.3 | 16.5±2.2 | 6.5±1.8 |
| 15 Gy | 0 | 52.6±5.2 | 37.4±3.5 | 10.1±0.8 |
| | 3 | 49.9±4.1 | 35.8±4.3 | 14.2±2.3 |
| | 4 | 18.9±4.2 | 21.1±2.6 | 60.0±6.3 |
| | 5 | 21.0±3.5 | 13.0±1.3 | 66.0±5.3 |
| | 6 | 20.7±2.5 | 12.9±1.3 | 66.4±3.0 |

[a]The values represent the means and the standard deviations of three separate experiments ($p<0.05$).

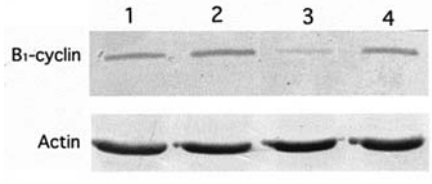


Figure 5. Western blot analysis of $B_1$-cyclin (62 kDa) expression in HT-29 late spheroids. Control late spheroids after 4 days of growth (lane 1); late spheroids after 24 h of irradiation (lane 2); control late spheroids after 5 days of growth (lane 3); late spheroids 48 h after irradiation (lane 4). As can be seen in lanes 2 and 4, late spheroids show an accumulation of $B_1$-cyclin protein indicative of $G_2$ cycle arrest. Conversely, control spheroids after 4 and 5 days of growth (lanes 1 and 3) are characterized by a decrease of the same protein due to cell cycle progression. An anti-actin antibody was used to identify variations in total protein amounts. Fifty $\mu$g of protein per lane, obtained from whole-cell extracts, was subjected to blot analysis using antibodies against $B_1$-cyclin. One of three separate experiments is presented.

days of growth (Fig. 5, lanes 1 and 3) are characterized by a decrease of the same protein due to cell cycle progression.

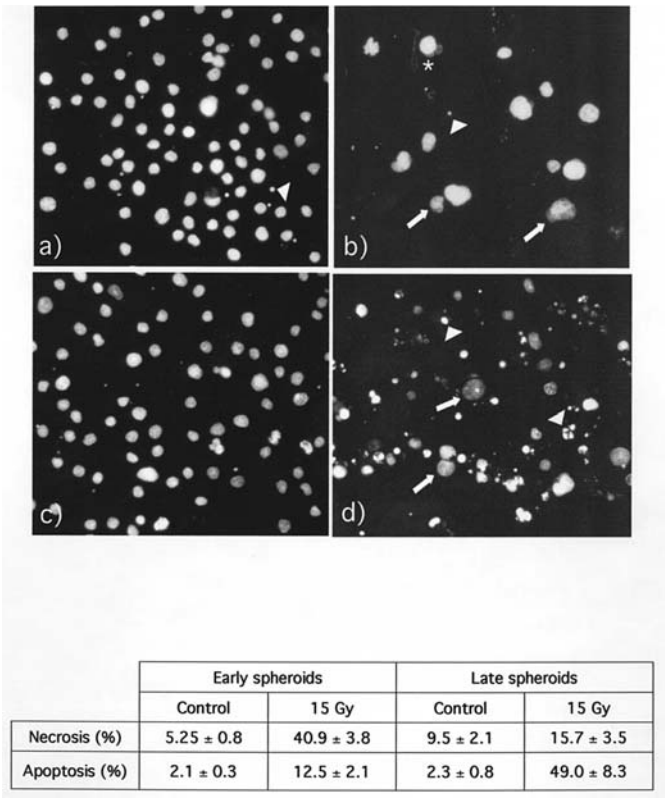


| | Early spheroids | | Late spheroids | |
|---|---|---|---|---|
| | Control | 15 Gy | Control | 15 Gy |
| Necrosis (%) | 5.25 ± 0.8 | 40.9 ± 3.8 | 9.5 ± 2.1 | 15.7 ± 3.5 |
| Apoptosis (%) | 2.1 ± 0.3 | 12.5 ± 2.1 | 2.3 ± 0.8 | 49.0 ± 8.3 |

Figure 6. Representative fluorescence micrographs of disaggregated Hoechst-stained single cells from control early spheroids after 72 h of growth (a) and early spheroids 48 h after irradiation (b). Control late spheroids after 5 days of growth (c) and late spheroids 48 h after irradiation (d) are also shown. Nuclei of control cells from both early and late spheroids (a and c, respectivley) have a uniformly organized chromatin even though some apoptotic cells are present (arrowheads). In early spheroids 48 h after irradiation (b), most of the nuclei have shrunken and/or disintegrated chromatin, typical of necrosis (arrows). In addition, many nuclei are enlarged and some present blebs on their surfaces (asterisk). Late spheroids 48 h after irradiation (d), present condensed and/or marginalized chromatin typical of apoptotic cells (arrowheads). A few necrotic nuclei were also present (arrows). The quantitative analysis of necrosis and apoptosis is shown in the table at the bottom of the figure. The percentages represent the means and the standard deviations of three separate experiments ($p<0.05$). Original magnification x1250.

*Analysis of cell death*. It is well known that the type of cell death induced by ionizing radiation is strictly associated with the cell cycle arrest checkpoint (12,13). Therefore, in order to verify that in fact apoptosis in late spheroids was associated with the $G_2/M$ cell cycle arrest checkpoint, and that necrosis in early spheroids was not related to any cell cycle arrest, the nuclear dye Hoechst was used to determine the type of cell death. In Fig. 6, nuclei of cells from control spheroids and from early and late spheroids, respectively, taken after 48 h from irradiation are shown. As can be seen in Fig. 6a and c, nuclei of control cells from both early and late spheroids have a uniformly organized chromatin even if low percentages of apoptotic cells are present (arrowheads). On the other hand, nuclei of early spheroids 48 h from irradiation (Fig. 6b) appear greatly damaged. Most of the nuclei have shrunken and/or show disintegrated chromatin, typical of necrosis (Fig. 6b, arrows). In addition, many nuclei are enlarged and some present blebs on their surfaces (Fig. 6b, asterisk). The quantitative analysis at the bottom of the Fig. 6 demonstrates

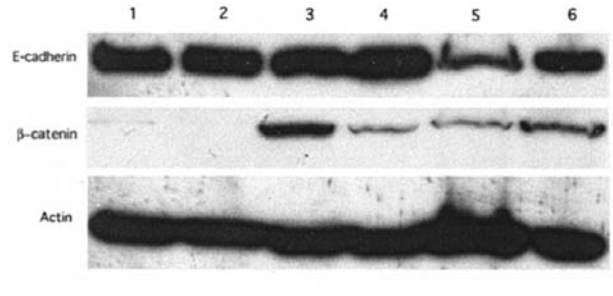


Figure 7. Western blot analysis of E-cadherin (120 kDa) and ß-catenin (95 kDa) expression and localization in HT-29 early and late spheroids. Total cell extracts of early spheroids (lane 1), total cell extracts of late spheroids (lane 2), Triton X-100-soluble fractions of early spheroids (lane 3), Triton X-100-soluble fractions of late spheroids (lane 4), Triton X-100-insoluble fractions of early spheroids (lane 5) and Triton X-100-insoluble fractions of late spheroids (lane 6). The total cell extracts of both early and late spheroids contain the same amount of E-cadherin whereas Triton X-100-isoluble fractions of late spheroids contain greater amounts of both E-cadherin and ß-catenin proteins. An anti-actin antibody was used to identify variations in total protein amounts. Fifty $\mu$g of protein per lane, obtained from cell extracts, were subjected to blot analysis using antibodies against E-cadherin and ß-catenin. One of three separate experiments is presented.

that about 40.9% of the cells are necrotic. When late spheroids were observed 48 h from irradiation, condensed and/or marginalized chromatin typical of apoptotic cells (Fig. 6, arrowheads) was noted. A few necrotic nuclei could also be observed (Fig. 6, arrows). The quantitative analysis reveals that about 49.0% of cells are apoptotic. From these results, it can be concluded that the same dose of ionizing radiation is able to induce necrosis in early spheroids and apoptosis in late, more compacted spheroids.

*Analysis of E-cadherin/ß-catenin expression and distribution.* In order to analyze the mechanisms by which the different degree of compaction of early and late spheroids could be accountable for their different response to the same dose of γ-rays, E-cadherin and ß-catenin expression and cellular distribution were determined by Western blot analysis (Fig. 7). It should be recalled that E-cadherin, together with its cytoplasmic partner ß-catenin, plays a pivotal role in determining the strength of cellular adhesion as well as providing survival signals to anchorage-deprived cells (14,15). As can be seen in Fig. 7, whole cell extracts of early (lane 1) and late (lane 2) spheroids contain the same amount of E-cadherin. However, when E-cadherin was analyzed in the different cell fractions (i.e., cell membrane/cytoplasm or TX-100 soluble fraction and nuclear/cytoskeleton or TX-100 insoluble fraction), a different pattern was observed. In fact, late spheroids contain a greater amount of E-cadherin in the TX-100 insoluble fraction (Fig. 7, lane 6) indicative of a stronger connection between E-cadherin and the cytoskeleton than early spheroids. In addition, ß-catenin is also more abundant in the TX-insoluble fraction of late spheroids (Fig. 7, lane 6) than of that of early spheroids (Fig. 7, lane 5). These data suggest that E-cadherin and ß-cateninn form a membrane complex connected to the cytoskeleton which may serve to strengthen cell-cell adhesion and, consequently, spheroid compaction.

## Discussion

The data presented in this report seem to indicate that the degree of cell compaction can influence the response of multicellular tumor spheroids to ionizing radiation. In particular, HT-29 well-compacted spheroids (late spheroids) appear to be more resistant than loose spheroids (early spheroids). The morphological analysis of early spheroids conducted 48 h after irradiation reveals massive damage as evidenced by the destruction of their three-dimensional organization and by plasma membrane blebbing. Conversely, late spheroids after irradiation show a well-preserved spatial array similar to controls. In addition to these morphological observations, other cell parameters also indicate an increase in resistance in late spheroids. In fact, cell cycle and cell death analyses demonstrate a different mechanism of response to 15 Gy of γ-rays in early and late spheroids. Specifically, the absence of cell cycle delay and the onset of necrosis were revealed in early irradiated spheroids, while an evident $G_2$/M cell cycle arrest and the onset of apoptosis were present in late spheroids after irradiation.

How can these two different types of responses be considered signs of a diverse degree of resistance? In order to answer this question, it is necessary to recall that the same antitumor agent (e.g., ionizing radiation) can induce either necrosis or apoptosis in the same cellular system depending on the dose used (16-18). In particular, it has been demonstrated that high doses of ionizing radiation can induce necrosis whereas low doses can induce apoptosis. Furthermore, necrosis and apoptosis are two very different forms of cell death (19,20). Necrosis is defined as an accidental form of death which occurs when cells are so damaged that no active response to that damage is triggered (20,21). As a result of these great injuries, the cell membrane and, consequently, cell structure collapse (22). On the contrary, apoptosis is a well-regulated mechanism of cell death that occurs when the damage induced is not so massive to exclude the possibility that repair mechanisms are at least triggered (22). It is hypothesized that cell cycle arrest at the $G_0/G_1$ or $G_2$/M checkpoints is a damage repair strategy (23). If repair is successful, cells go on in their proliferation activity. If not, signals necessary for apoptosis through the activation of proteins involved in a selective destruction of cellular compartments (nucleus, membrane, etc.) are generated (24,25). With this in mind, it can be postulated that, in late spheroids, the cell cycle is blocked at the $G_2$/M checkpoint and damage repair is attempted. However, since these spheroids die of apoptosis, it can be deduced that repair is not successful and, consequently, the cells die. On the contrary, it can be hypothesized that damage is so great in early spheroids that no repair is attempted and, consequently, the spheroids undergo necrosis. For these reasons, early spheroids are more sensitive than late spheroids to the same dose of ionizing radiation.

Various hypotheses may be formulated to explain the difference in resistance to ionizing radiation observed in early and late spheroids. It has been suggested that cell cycle distribution may be responsible for differences in resistance (26). These investigators demonstrated that the resistance of compact spheroids to both antineoplastic drugs and ionizing

radiation differs with respect to that of loose spheroids and linked this resistance to the different cell cycle distributions of the two spheroid models. They demonstrated that about 80-90% of cells in compact resistant spheroids were arrested in the $G_1$ phase of cell cycle. Therefore, the authors hypothesized that this arrest could render cells less susceptible to drug- and radiation-induced damage (e.g., due to DNA conformation) and, consequently, could be responsible for the observed resistance. They also showed that the cyclin-dependent kinase inhibitor p27 could be the mediator of the resistance observed in compact spheroids. The reduction of p27 levels obtained through the use of specific antisense oligonucleotides was accompanied by an increase in proliferation and in drug sensitivity. The authors also concluded that the cell-cell adhesion molecule E-cadherin could be involved in the increase of p27 in compact resistant spheroids (27). With these results in mind, it can also be speculated that the data presented in the present report confirm that the compaction of HT-29 spheroids is related to an increase in resistance to ionizing radiation. However, since cell cycle analyses in the present study revealed no important differences in cell cycle distribution in early and late spheroids before irradiation, the involvement of cell cycle distribution appears not to be responsible for the differences observed in resistance. For this reason, another explanation for compaction-induced resistance of late spheroids should be sought.

It can be suggested that the changes in spheroid architecture which lead to compaction could arise by the different expression of molecules involved in cell-cell and/or cell-matrix interactions. Possible candidates include cell adhesion molecules (CAMs), components of the extracellular matrix (ECM) and gap junctional components. As far as CAMs are concerned, particularly important could be the role played by cadherins. Cadherins belong to a class of trans-membrane proteins that are involved mainly in intercellular adhesion (14) and directly influence the strength of adhesive interaction between cells (28). The intercellular interactions mediated by cadherins are diverse and include cohesion of cells, tissue segregation, epithelia formation and the preservation of tissue architecture in developing organisms (29). Furthermore, cadherins play an important role also in tumor progression. It has been demonstrated that E-cadherin together with its cytoplasmic partners, α-, ß-, and γ-catenins, regulate the strength of adhesion between tumor cells and the invasive properties of cancer cells both *in vitro* and *in vivo* (30,31).

It is well known from numerous studies in the literature that the expression and the distribution of E-cadherin/catenin complexes on plasma membranes play an important role in determining the strength of cell adhesion and tissue compaction. For example, in a very elegant study Adams and coworkers analyzed the mechanism by which E-cadherin and catenins associate with each other and strengthen the adhesion between epithelial cells (32). They used time-lapse differential interference contrast (DIC) imaging to demonstrate that the pool of E-cadherin and catenins resistant to the extraction with Triton X-100 (TX-100 insoluble fraction) is critical for cell-cell adhesion. They also revealed that the TX-100 fraction is strictly associated with the actin cytoskeleton and accumulates rapidly at cell-cell contact sites called puncta. The authors concluded that the concentration of E-cadherin/catenin complexes or puncta may be important for strengthening adhesion between cells. The importance of the redistribution of the cadherin/catenin complex on the plasma membrane in determining the strength of cell adhesion was also demonstrated by Monier-Gavelle and Duband (33). They showed that the clustering of neural cells, obtained through a selective inhibition of cell adhesion onto ECM components, was not mediated by the overexpression of N-cadherin/catenin complex, but by its redistribution on the plasma membrane. Western blot analysis revealed that the TX-100 fraction of cells organized in clusters contained a higher amount of the N-cadherin/catenin complex with respect to monolayers. These results illustrate that the redistribution of N-cadherin/catenin complexes on the plasma membrane is very important in determining the strength of adhesion in cells that are no longer able to attach to the substratum.

It should also be recalled that cadherins play a pivotal role not only in reinforcing cell-cell adhesion, but also in transducing signals inside the cell (14,34). In particular, it has been demonstrated that E-cadherin was able to provide survival signals in squamous carcinoma cells grown in an anchorage-independent way (15) (i.e., as aggregates). The authors postulated that the crucial event during cadherin-mediated anchorage-independent growth was the process of compaction. They observed that this process was similar to the one occurring during blastocyst formation that was due to the active contraction of the actin cytoskeleton tethered to cadherin/catenin complexes.

Given the evident importance of E-cadherin in determining the compaction of cell aggregates and given its critical role in providing survival signals in cell clusters, E-cadherin/ß-catenin complex expression and distribution on plasma membranes of HT-29 cells in early and late spheroids were also analyzed in the present study by Western blotting. The results reveal that early and late spheroids express the same amount of E-cadherin, but that the TX-100 insoluble fraction of late compact spheroids contains a higher amount of E-cadherin and ß-catenin than early loose spheroids. From these results, it can be hypothesized that the compaction of late spheroids may not be the result of E-cadherin protein over-expression, but rather of its re-arrangement on the plasma membrane of HT-29 cells. The higher amounts of E-cadherin and ß-catenin in the TX-100 insoluble fraction of late spheroids may be indicative of a tight connection between E-cadherin and actin through the engagement of cytoplasmic ß-catenin. It can be speculated that the connection of these complexes to the cytoskeleton may be critical to strengthening the adhesion between cells and, consequently, in determining the compaction of HT-29 late spheroids.

In conclusion, from the data presented herein, it can be suggested that the compaction of late HT-29 spheroids may play a role in determining their increased resistance to ionizing radiation. It can also be speculated that the molecular mechanisms responsible for the compaction-induced resistance of HT-29 spheroids could be mediated by the redistribution of E-cadherin/ß-catenin complexes on the plasma membrane.

## References


1. Inch WR, McCredie JA and Sutherland RM: Growth of nodular carcinomas in rodents compared with multi-cell spheroids in tissue culture. Growth 34: 271-282, 1970.
2. Sutherland RM, McCredie JA and Inch WR: Growth of multicell spheroids in tissue culture as a model of nodular carcinomas. J Natl Cancer Inst 46: 113-120, 1971.
3. Olive PL and Durand RE: Drug and radiation resistance in spheroids: cell contact and kinetics. Cancer Metastasis Rev 13: 121-138, 1994.
4. Kerbel RS, Rak J, Kobayashi H, Man MS, St Croix B and Graham CH: Multicellular resistance: a new paradigm to explain aspects of acquired drug resistance of solid tumors. Cold Spring Harb Symp Quant Biol 59: 661-673, 1994.
5. Bates RC, Buret A, van Helde DF, Harton MA and Burns RC: Apoptosis induced by inhibition of intercellular contact. J Cell Biol 125: 403-415, 1994.
6. Durand RE and Sutherland RM: Effects of intercellular contact on repair of radiation damage. Exp Cell Res 71: 75-80, 1972.
7. Bär PR: Apoptosis - the cell's silent exit. Life Sci 59: 369-378, 1996.
8. Oberhammer FA, Froschl G, Tiefenbacher R, *et al*: A topical issue of microscopy research and technique. Microsc Res Tech 34: 247-258, 1996.
9. Inayat-Hussain SH, Cohen GM and Cain K: A reappraisal of the role of $Zi^{++}$ in TGF-ß1-induced apoptosis in primary hepatocytes. Cell Biol Toxicol 15: 381-387, 1999.
10. Sasaki CY, Lin H and Passaniti A: Expression of E-cadherin reduces Bcl-2 expression and increases sensitivity to etoposide-induced apoptosis. Int J Cancer 86: 660-666, 2000.
11. Tamamoto T, Ohishi K, Takahashi A, Wang X, Yosimura H, Ohishi H, Uchida H and Ohnishi T: Correlation between γ-ray-induced G2 arrest and radioresistance in two human cancer cells. Int J Radiat Oncol Biol Phys 44: 905-909, 1999.
12. Filippovich IV, Sorokina NI, Robillard N and Chatal JF: Radiation induced apoptosis in human ovarian carcinoma cells growing as monolayer and as multicell spheroids. Int J Cancer 72: 851-859, 1997.
13. Ling CC, Guo M, Chen CH and Deloherey T: Radiation-induced apoptosis: effects of cell age and dose fractionation. Cancer Res 55: 5207-5212, 1995.
14. Vleminckx K and Kemler R: Cadherins and tissue formation: integrating adhesion and signaling. Bioessays 21: 211-220, 1999.
15. Kantak SS and Kramer RH: E-cadherin regulates anchorage-independent growth and survival in oral squamous cell carcinoma cells. J Biol Chem 27: 16953-16961, 1998.
16. Akagi Y, Ito K and Sawada S: Radiation-induced apoptosis and necrosis in Molt-4 cells: a study of dose-effect relationships and their modification. J Radiat Biol 64: 47-56, 1993.
17. Lennon SV, Martin SJ and Cotter TG: Induction of apoptosis (programmed cell death) in tumor cell lines by widely diverging stimuli. Biochem Soc Trans 18: 343-345, 1990.
18. Lennon SV, Martin SJ and Cotter TG: Dose-dependent induction of apoptosis in human tumor cell by widely diverging stimuli. Cell Prolif 24: 203-214, 1991.
19. Nelson DA and White E: Exploiting different ways to die. Genes Dev 18: 1223-1226, 2004.
20. Okada H and Mak TW: Pathways of apoptotic and non-apoptotic death in tumor cells. Nat Rev Cancer 4: 592-603, 2004.
21. Boonstra J and Post JA: Molecular events associated with reactive oxygen species and cell cycle progression in mammalian cells. Gene 337: 1-13, 2004.
22. Ziegler U and Groscurth P: Morphological features of cell death. N Physiol Sci 19: 124-128, 2004.
23. Pawlik TM and Keyoparsi KK: Role of cell cycle in mediating sensitivity to radiotherapy. Int J Radiat Oncol Biol Phys 59: 928-942, 2004.
24. Schmidt-Ullrich RK, Dent P, Grant S, Mikkelsen RB and Valerie K: Signal transduction and cellular radiation responses. Radiat Res 153: 245-257, 2000.
25. Vermeulen K, Berneman ZN and van Bockstaele DR: Cell cycle and apoptosis. Cell Prolif 36: 165-175, 2003.
26. St Croix B, Florens VA, Rak JV, Flanagan M, Bhattacharya N, Slingerland JM and Kerbel RS: Impact of the cyclin dependent kinase inhibitor $p27^{Kip1}$ on adhesion-dependent resistance of tumor cells to anticancer agents. Nat Med 2: 1204-1210, 1996.
27. St Croix B, Sheehan C, Rak JW, Florenes VA, Slingerland JM and Kerbel RS: E-Cadherin-dependent growth suppression is mediated by the cyclin-dependent kinase inhibitor p27(KIP1). J Cell Biol 142: 557-571, 1998.
28. Steinberg MS and Takeichi M: Experimental specification of cell sorting, tissue spreading and specific spatial patterning by quantitative differences in cadherin expression. Proc Natl Acad Sci USA 91: 206-209, 1994.
29. Yap AS, Brieher WM, Pruschy M and Gumbiner BM: Lateral clustering of the adhesive ectodomain: a fundamental determinant of cadherin function. Curr Biol 7: 308-315, 1997.
30. Margulis A, Zhang W, Alt-Holland A, Crawford HC, Fusening NE and Garlick JA: E-cadherin suppression accelerates squamous cell carcinoma progression in three-dimensional, human tissue constructs. Cancer Res 65: 1783-1791, 2005.
31. Awaya H, Takeshima Y, Amatya VJ, Ishida H, Yamasaki M, Kohno N and Inai K: Loss of expression of E-cadherin and beta-catenin is associated with progression of pulmonary adenocarcinoma. Pathol Int 55: 14-18, 2005.
32. Adams CL, Nelson WJ and Smith S: Quantitative analysis of cadherin-catenin-actin reorganization during development of cell-cell adhesion. J Cell Biol 135: 1899-1911, 1996.
33. Monier-Gavelle F and Duband JL: Cross talk between adhesion molecules: control of N-cadherin activity by intracellular signals elicited by b1and b3 integrins in migrating neural crest cells. J Cell Biol 137: 1663-1681, 1997.
34. Behrens J: Cadherins and catenins: role in signal tranduction and tumor progression. Cancer Metastasis Rev 18: 15-30, 1999.